Annals of Glaciology 35 2002

Distribution of oxygen isotope ratios and snow accumulation rates in Wilhelm II Land, East Antarctica

BARBARA T. SMITH, TAS D. VAN OMMEN, VIN I. MORGAN
Antarctic CRC and Australian Antarctic Division, Box 252-80, Hobart, Tasmania 7001, Australia
E-mail: barbara.smith@utas.edu.au

ABSTRACT. Records of recent oxygen isotope ratios ($\delta^{18}O$) and accumulation rates are presented for the region of Wilhelm II Land, East Antarctica, between 78° and 93° E and from the coast to 2100 m elevation. These records were derived from analysis of 21 shallow firn cores collected during the 1997/98 and 1998/99 Australian National Antarctic Research Expeditions summer operations. The accumulation rates were determined using comparisons between detailed analyses of density, $\delta^{18}O$, hydrogen peroxide (H_2O_2) levels and electrical conductivity. The $\delta^{18}O$ distribution follows an approximately linear relationship with snow surface elevation, with values from −22‰ near the coast to −32‰ towards 2000 m elevation. Accumulation-rate distribution does not display this simple relationship with topography. South of the West Ice Shelf the contours run parallel to lines of latitude (oblique to the coast and topography), with 400 kg m^{-2} a^{-1} towards the coast and 2000 m elevation, and a lower zone of 300 kg m^{-2} a^{-1} along an axis of 68.4° S. This pattern of accumulation is also evident along the Mirny–Vostok traverse route. Southwest of the West Ice Shelf the rate of accumulation drops gradually from 300 to 200 kg m^{-2} a^{-1} towards Lambert Glacier basin. Surface-snow redistribution and variations in accumulation rate cause variability in the clarity of core records, but several sites show sufficient stratigraphic preservation to suggest potential for extraction of extended palaeoenvironmental records through further drilling.

INTRODUCTION

Wilhelm II Land lies between Davis and Mirny stations in East Antarctica (78–93° E) and until recently has not been studied in detail. This paper summarizes the results from shallow-firn-core analysis from this area, and outlines the potential for further drilling investigations. A full data report is in Smith and others (2001).

SAMPLING AND ANALYSIS

Twenty-one shallow firn cores were collected at 500–2100 m elevation during the 1997/98 and 1998/99 Australian National Antarctic Research Expeditions (ANARE) summer expeditions (Table 1; Fig. 1). A Polar Ice Coring Office (PICO) hand auger was used to collect 20 cores of approximately 5 m length, and one 10 m core at site Mount Brown South (MBS) where an automatic weather station was installed.

The cores from the 1997/98 season were sampled and measured for electrical conductivity (EC) at the Co-operative Research Centre for the Antarctic and Southern Ocean Environment (Antarctic CRC) in Hobart, and the cores from the 1998/99 season were sampled and measured for EC and density at Davis station. A density measurement was made for each of the latter core sections (each approximately 1 m long). All samples were analyzed for oxygen isotope ratio ($\delta^{18}O$) and hydrogen peroxide (H_2O_2) levels as contiguous 4 or 5 cm samples.

Accumulation rates were determined for each site by identification of annual layers within the $\delta^{18}O$, H_2O_2 and EC records. An example of one core (U5) is presented in Figure

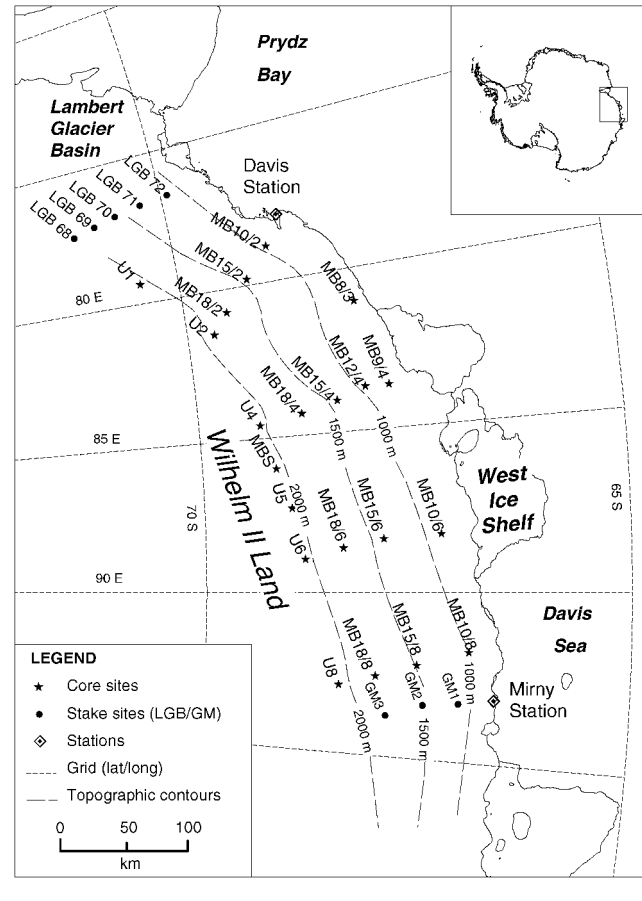

Fig. 1. Location of shallow firn-core sites in Wilhelm II Land (U and MB), and stake sites along the Lambert Glacier basin traverse route (LGB sites) and along the Mirny–Dome C traverse route (GM sites), East Antarctica.

https://doi.org/10.3189/172756402781816898 Published online by Cambridge University Press

Table 1. Shallow-core and stake-site information in and near Wilhelm II Land including positions, $\delta^{18}O$, accumulation rates and epochs (LGB sites from Higham and Craven, 1997; GM sites from Young, 1979)

Core sites*	Date of coring	Location	Elevation	Borehole depth	$\delta^{18}O$	Accumulation	Epoch
			m a.s.l.	m	‰	kg m^{-2} a^{-1}	
U1	6 Jan. 1998	−70.44540° S, 79.31669° E	2027	3.86	−32.04	197° ± 38	1988–97
MB10/2	31 Dec. 1998	−68.91032° S, 78.84991° E	915	5.13	−26.21	330° ± 44	1990–98
MB15/2	31 Dec. 1998	−69.20294° S, 79.78910° E	1430	5.13	−29.24	274° ± 42	1990–98
MB18/2	31 Dec. 1998	−69.49968° S, 80.74904° E	1747	5.13	−31.41	251° ± 21	1989–98
U2	6 Jan. 1998	−69.68240° S, 81.41640° E	1955	4.65	−31.83	352° ± 49	1991–97
MB8/3	7 Jan. 1999	−68.00382° S, 81.00394° E	598	4.93	−21.42	267° ± 38	1990–98
MB9/4	7 Jan. 1999	−67.72413° S, 83.65856° E	482	3.16	−24.78	368° ± 70	1995–98
MB12/4	7 Jan. 1999	−68.00547° S, 83.64908° E	966	5.01	−25.29	244° ± 18	1989–98
MB15/4	30 Dec. 1998	−68.35017° S, 83.99831° E	1411	4.97	−28.40	408° ± 60	1993–98
MB18/4	28 Dec. 1998	−68.77800° S, 84.30000° E	1800	6.15	−30.56	225° ± 20	1985–98
U4	6 Jan. 1998	−69.27876° S, 84.56459° E	2034	5.41	−34.27	461° ± 58	1992–97
MBS	23 Dec. 1998	−69.13097° S, 85.99853° E	2064	10.22	−32.82	255° ± 24	1979–98
U5	12 Jan. 1998	−68.97274° S, 87.29045° E	2034	5.49	−32.44	329° ± 44	1990–97
MB10/6	8 Jan. 1999	−67.23213° S, 88.24499° E	825	4.79	−22.99	442° ± 51	1993–98
MB15/6	8 Jan. 1999	−67.91095° S, 88.34569° E	1394	4.88	−29.37	383° ± 56	1992–98
MB18/6	8 Jan. 1999	−68.38879° S, 88.60341° E	1721	4.83	−31.89	242° ± 26	1989–98
U6	12 Jan. 1998	−68.83440° S, 88.93410° E	2036	6.00	−33.94	315° ± 33	1988–97
MB10/8	29 Dec. 1998	−66.91098° S, 91.75384° E	974	6.11	−24.04	461° ± 122	1993–98
MB15/8	29 Dec. 1998	−67.51802° S, 92.18551° E	1538	5.08	−27.60	238° ± 32	1988–98
MB18/8	29 Dec. 1998	−68.00060° S, 92.55763° E	1812	5.16	−30.51	324° ± 35	1991–98
U8	12 Jan. 1998	−68.42703° S, 92.86826° E	2067	4.96	−32.48	261° ± 30	1988–97
Stake sites – previous work							
LGB 72		−69.92089° S, 76.49334° E	1038		−28.30	282	1994–96
LGB 71		−70.25875° S, 76.68315° E	1387		−30.20	216	1994–96
LGB 70		−70.57571° S, 76.86641° E	1651		−30.60	229	1994–96
LGB 69		−70.83519° S, 77.07788° E	1854		−33.40	192	1994–96
LGB 68		−71.09538° S, 77.28863° E	1996		−34.90	187	1994–96
GM1		−67.01042° S,93.29259° E	914			420	1976–77
GM2		−67.42845° S,93.38443° E	1455			270	1976–77
GM3		−67.86002° S,93.75035° E	1758			230	1976–77

* Core sites listed from west to east and from low to high elevation.

2. Most of these records indicate reasonable agreement between the annual cycle positions, but the quality of the records varied (Smith and others, 2001). Snow stakes were also installed at most sites, and preliminary analysis of these data indicates that the accumulation rates defined through core analysis are generally consistent with the order of magnitude from stake measurements (Smith and others, 2001).

Temperature measurements were made in each borehole, but time restraints due to helicopter operations led to inaccurate data which have not been used in this study.

The $\delta^{18}O$ and accumulation datasets were contoured using Generic Mapping Tools (GMT) software with an adjustable tension surface and a grid of $2^\circ \times 20'$ (longitude and latitude) (Smith and Wessel, 1990; Wessel and Smith, 1998). Where possible, data from Lambert Glacier basin (LGB) and Mirny–Dome C traverse routes have been incorporated into these maps (Table 1).

OXYGEN ISOTOPE DISTRIBUTION

The average $\delta^{18}O$ values for each site were determined by a simple average of all samples in one core. Each core covered more than three annual layers, so the average $\delta^{18}O$ values are assumed to lie within 1‰ of the recent annual mean (Morgan, 1982). These values are contoured in Figure 3 with additional data from individual stake sites along the LGB traverse route (Higham and Craven, 1997; Table 1). The contour distribution in Figure 3 shows that $\delta^{18}O$ and topographic contours are approximately parallel, with $\delta^{18}O$ values decreasing linearly with increasing elevation at a rate of approximately −1‰ per 125 m elevation. The −22‰ contour is inferred to be near the coast, and −32‰ towards 2000 m elevation.

These new data fill a gap in the compilations of Morgan (1982) and Qin and others (1994), both of which were used by Giovinetto and Zwally (1997) and Zwally and others (1998) to construct model distributions. The main difference between the respective distribution patterns is the position of the −20‰ contour in the vicinity of the grounding line of the West Ice Shelf. In Morgan (1982) this contour is on the continent, while later distribution patterns agree that this contour is on the West Ice Shelf. This latter result implies a significant continentality effect by the West Ice Shelf.

ACCUMULATION

Accumulation data from adjacent areas (LGB and Mirny–Dome C traverse routes; Young, 1979; Higham and Craven, 1997) were assimilated with data from this project for contouring as shown in Figure 4. In contrast to the $\delta^{18}O$ contour pattern, there is no simple relationship between accumulation rate and elevation. Between 82° and 94° E the accumulation-rate contours run approximately parallel to lines of latitude and therefore oblique to the coast. Near

https://doi.org/10.3189/172756402781816898 Published online by Cambridge University Press

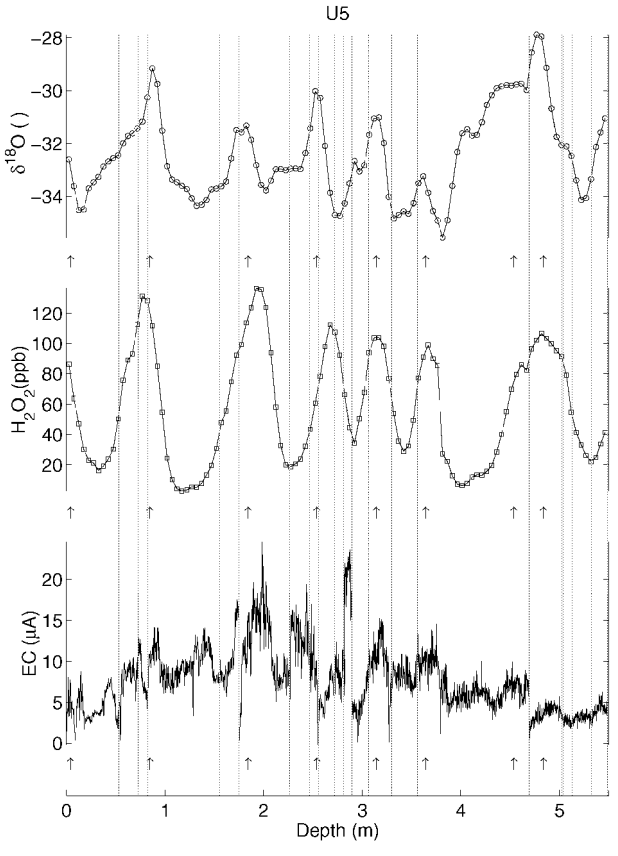

Fig. 2. An example of $\delta^{18}O$, H_2O_2 and EC measurement analyses (core U5). Arrows indicate where summer peaks have been identified and used to define the accumulation rate.

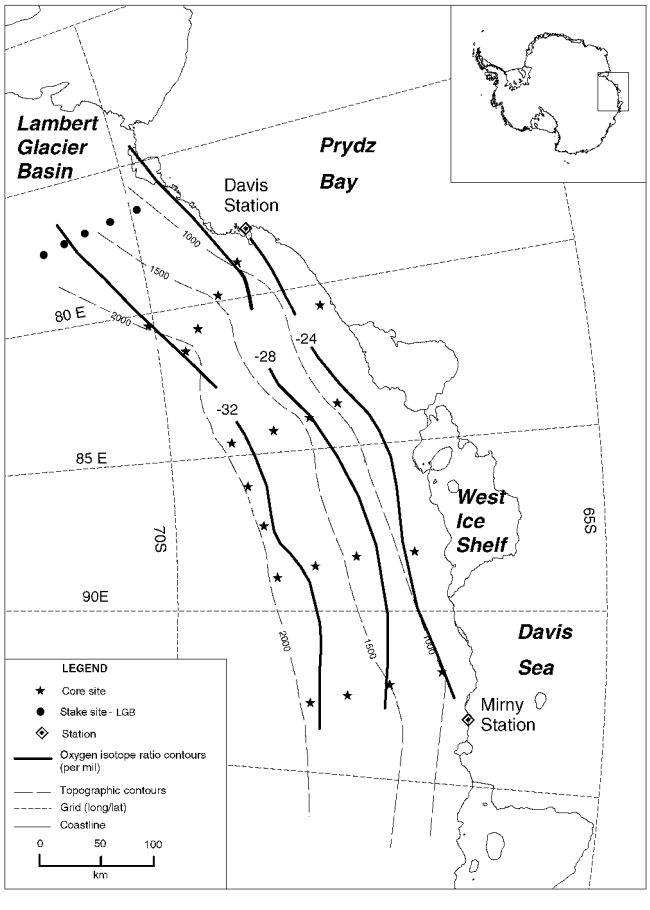

Fig. 3. $\delta^{18}O$ contours showing distribution approximately parallel to topography, from −22‰ inferred near the coast to −32‰ towards 2000 m elevation (see Fig. 1 for site names, and Table 1 for site values).

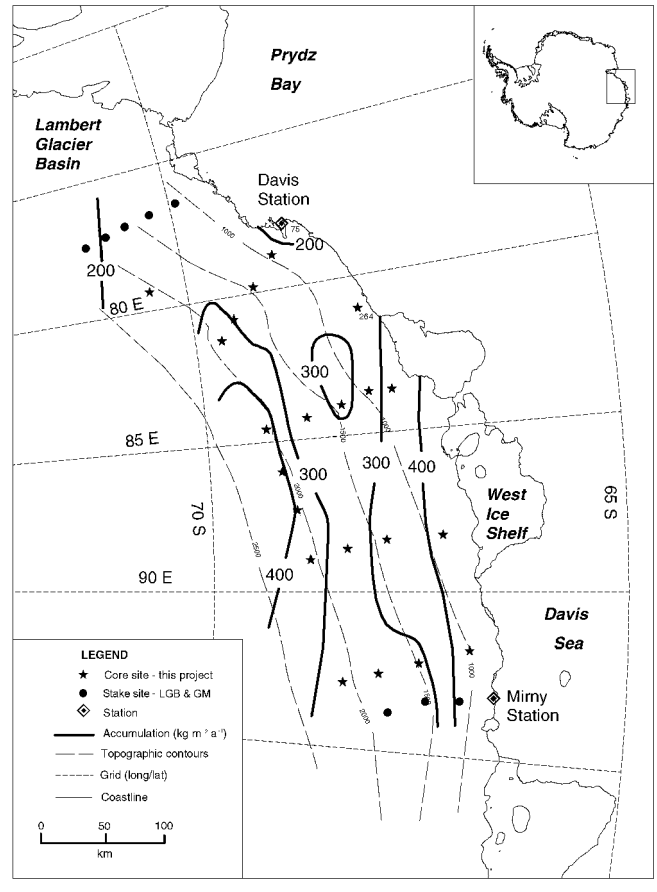

Fig. 4. Accumulation-rate contours showing a zone of relatively low accumulation rate of 300 kg m^{-2} a^{-1} along an axis of 68.4° S, compared with the coast near the West Ice Shelf and 2000 m elevation where the rate is 400 kg m^{-2} a^{-1}. Towards LGB to the west the accumulation rate falls steadily from 300 to 200 kg m^{-2} a^{-1}.

the West Ice Shelf the rate is 400 kg m^{-2} a^{-1}, but it falls steadily to 300 kg m^{-2} a^{-1}, forming a zone of relatively low accumulation with an axis along 68.4° S. Towards 69° S the rate rises back to 400 kg m^{-2} a^{-1}. West of 82° E the rates fall more steadily from 300 to 200 kg m^{-2} a^{-1} towards LGB.

DISCUSSION

Figure 5 presents several accumulation-rate profiles along the Mirny–Vostok and Mirny–Dome C traverse routes showing rates ranging from 400–800 kg m^{-2} a^{-1} at the coast to <50 kg m^{-2} a^{-1} at Vostok (1400 km inland). Accumulation rates have been measured periodically along this traverse for >30 years. Several profiles are included in Figure 5 to allow an appreciation of the variability between datasets. The profiles indicate two zones of accumulation relatively lower than the trend: 50–150 km and 230–350 km from the coast. Projection of a parallel line of data from this project (approximately 30 km to the west) on to the traverse line shows there is good correlation between datasets, with similar distribution and the same lower accumulation zone within 150 km of the coast.

Given the similar characteristics between the Mirny–Vostok traverse route and the data from this project, it is expected that the accumulation rates south of the sampled area (at least within 200 km of the Mirny–Vostok traverse

https://doi.org/10.3189/172756402781816898 Published online by Cambridge University Press

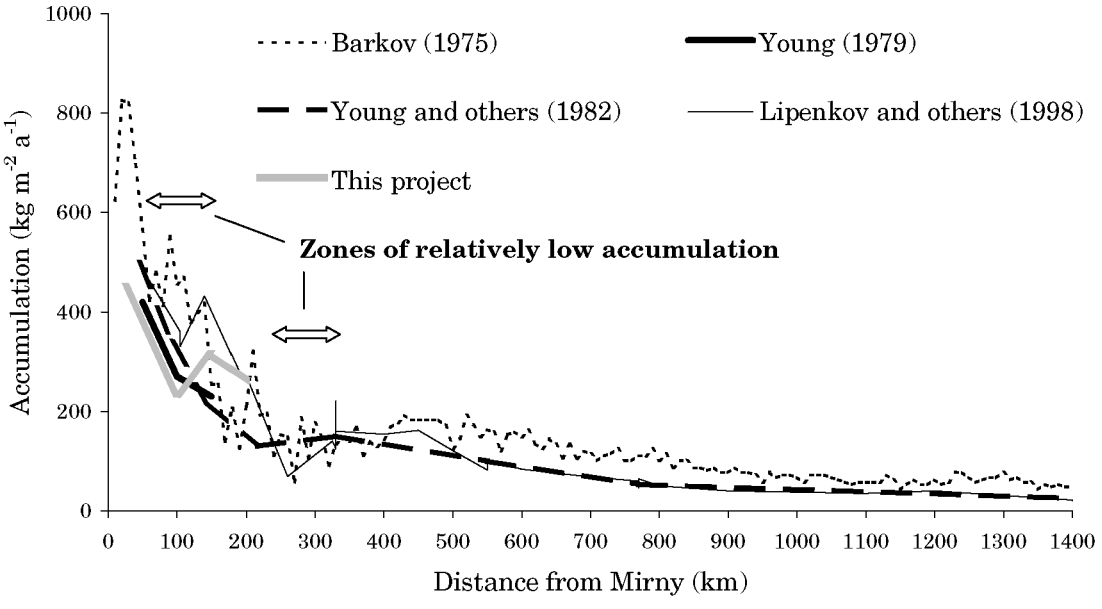

Fig. 5. Examples of accumulation rates along the Mirny–Vostok traverse route, showing two zones of relatively low accumulation between the coast and 400 km inland. Data from this project correlate with the outer zone of lower accumulation.

route) follow a similar pattern. Further sampling is required to confirm this suggestion.

Accumulation-rate distribution is believed to be influenced by the combined effects of surface wind outflow/inflow patterns and coastline morphology and interference of a standing wave in the atmospheric boundary layer that locally enhances and suppresses snowfall patterns as suggested by Pettré and others (1986). The trigger for this disturbance is thought to be the change from a gently sloping ice plateau to a relatively steep surface slope at about 2000 m elevation.

CONCLUSION

The $\delta^{18}O$ analysis from this investigation provides useful ground-truthing data for previous $\delta^{18}O$ models, and used in conjunction with H_2O_2 and EC records has been used to infer accumulation rates across this region with sparse prior data. The results compare well at the boundaries with other accumulation studies in areas nearby, and provide detail for future Antarctic accumulation maps.

The complete dataset in Smith and others (2001) indicates there is scope for further drilling at sites near Mount Brown (e.g. U5 in Fig. 2) where 1–2 century records could be derived as a contribution to the International Trans-Antarctic Scientific Expedition (ITASE; Mayewski and Goodwin, 1996) program. Such drilling could provide data from a region with no palaeo-records and may be useful in linking longer-term inland continental records to coastal/Southern Ocean records.

ACKNOWLEDGEMENTS

The authors would like to thank the field personnel A. Ruddell, M. King, R. Manson and the crews of Helicopters Australia.

REFERENCES

Barkov, N. I. 1975. Snow accumulation along the Mirny–Vostok profile, 1970–1973. *Antarct. J. U.S.*, **10**(2), 56–57.

Giovinetto, M.B. and H. J. Zwally. 1997. Areal distribution of the oxygen-isotope ratio in Antarctica: an assessment based on multivariate models. *Ann. Glaciol.*, **25**, 153–158.

Higham, M. and M. Craven. 1997. *Surface mass balance and snow surface properties from the Lambert Glacier basin traverses 1990–94.* Hobart, Tasmania, Cooperative Research Centre for the Antarctic and Southern Ocean Environment. (Research Report 9.)

Lipenkov, V. Ya., A. A. Yekaykin, N. I. Barkov and M. Purshe. 1998. O svyazi plotnosti poverkhnostnogo sloya snega v Antarktide so skorost'yu vetra [On the connection between density of surface ice layer in Antarctica with wind velocity]. *Mater. Glyatsiol. Issled./Data Glaciol. Stud.* 85, 148–158.

Mayewski, P. A. and I. D. Goodwin, *comps*. 1996. *International Trans-Antarctic Scientific Expedition (ITASE). "200 years of past Antarctic climate and environmental change" Science and implementation plan, 1996. Report from the ITASE Workshop, Cambridge, United Kingdom, 2–3 August, 1996.* Durham, NH, University of New Hampshire. IGBP, SCAR. (PAGES Workshop Report 97-1.)

Morgan, V. I. 1982. Antarctic ice sheet surface oxygen isotope values. *J. Glaciol.*, **28**(99), 315–323.

Pettré, P., J. F. Pinglot, M. Pourchet and L. Reynaud. 1986. Accumulation distribution in Terre Adélie, Antarctica: effect of meteorological parameters. *J. Glaciol.*, **32**(112), 486–500.

Qin Dahe, J. R. Petit, J. Jouzel and M. Stievenard. 1994. Distribution of stable isotopes in surface snow along the route of the 1990 International Trans-Antarctica Expedition. *J. Glaciol.*, **40**(134), 107–118.

Smith, B.T. and A. Ruddell. 2001. *Snow accumulation in Wilhelm II Land, East Antarctica.* Hobart, Tasmania, Cooperative Research Centre for the Antarctic and Southern Ocean Environment. (Report 22.)

Smith, W. and P. Wessel. 1990. Gridding with continuous curvature splines in tension. *Geophysics*, **55**(3), 293–305.

Wessel, P. and W. H. F. Smith. 1998. New, improved version of the Generic Mapping Tools released. *Eos*, **79**(47), 579.

Young, N.W. 1979. Measured velocities of interior East Antarctica and the state of mass balance within the I.A.G.P. area. *J. Glaciol.*, **24**(90), 77–87.

Young, N.W., M. Pourchet, V. M. Kotlyakov, P. A. Korolev and M. B. Dyurgerov. 1982. Accumulation distribution in the IAGP area, Antarctica: 90° E–150° E. *Ann. Glaciol.*, **3**, 333–338.

Zwally, H.J., M. Giovinetto, M. Craven, V. Morgan and I. Goodwin. 1998. Areal distribution of the oxygen-isotope ratio in Antarctica: comparison of results based on field and remotely sensed data. *Ann. Glaciol.*, **27**, 583–590.

https://doi.org/10.3189/172756402781816898 Published online by Cambridge University Press